# AFOSR FINAL REPORT

**Principal Investigator:**

Jonathan Poggie
Professor
School of Aeronautics and Astronautics
Purdue University
West Lafayette IN 47906
jpoggie@purdue.edu
(765) 496-0614

**Project Title:**

Unsteady Separation: Mechanism and Mitigation

**Grant Number:**

FA9550-17-1-0153

**Period of Performance:**

February 2017 to September 2020

**Report Date:**

November 10, 2020

# REPORT DOCUMENTATION PAGE

*Form Approved*
*OMB No. 0704-0188*



| 1. REPORT DATE *(DD-MM-YYYY)* | 2. REPORT TYPE | 3. DATES COVERED *(From - To)* |
|---|---|---|
| 10-11-2020 | Final Report | 01-02-2017 to 01-09-2020 |

**4. TITLE AND SUBTITLE**
Unsteady Separation: Mechanism and Mitigation

**5a. CONTRACT NUMBER**

**5b. GRANT NUMBER**
FA9550-17-1-0153

**5c. PROGRAM ELEMENT NUMBER**

**6. AUTHOR(S)**
Jonathan Poggie

**5d. PROJECT NUMBER**

**5e. TASK NUMBER**

**5f. WORK UNIT NUMBER**

**7. PERFORMING ORGANIZATION NAME(S) AND ADDRESS(ES)**
School of Aeronautics and Astronautics, Purdue University
701 W Stadium Ave
West Lafayette IN 47907-2045

**8. PERFORMING ORGANIZATION REPORT NUMBER**

**9. SPONSORING/MONITORING AGENCY NAME(S) AND ADDRESS(ES)**
Air Force Office of Scientific Research
875 N Randolph St Room 3112
Arlington VA 22203

**10. SPONSOR/MONITOR'S ACRONYM(S)**
AFRL/AFOSR

**11. SPONSOR/MONITOR'S REPORT NUMBER(S)**

**12. DISTRIBUTION/AVAILABILITY STATEMENT**
Distribution A: Unlimited Distribution

**13. SUPPLEMENTARY NOTES**

**14. ABSTRACT**

For a compressible, turbulent compression ramp flow, this project demonstrated upstream influence on separation unsteadiness, selective response of separation motion to controlled upstream disturbances, and strong effects of confining sidewalls. The results support a model of separation unsteadiness in which external forcing by boundary layer turbulence drives a weakly-damped global mode of the separation bubble. This case was termed a damped resonator; it represents an intermediate case between instabilities that can be characterized by amplifier or oscillator models. Effective flow control appears achievable by matching actuator-induced perturbations to the global mode of the separation bubble.

**15. SUBJECT TERMS**
compressible turbulent flow, separation unsteadiness, flow control

| 16. SECURITY CLASSIFICATION OF: | | | 17. LIMITATION OF ABSTRACT | 18. NUMBER OF PAGES | 19a. NAME OF RESPONSIBLE PERSON |
|---|---|---|---|---|---|
| a. REPORT | b. ABSTRACT | c. THIS PAGE | | | 19b. TELEPHONE NUMBER *(Include area code)* |
| U | U | U | UU | | |

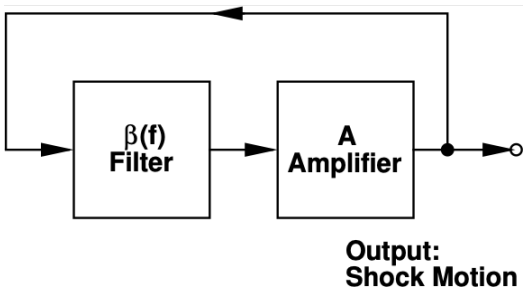


(a) Oscillator model: self-excited oscillations.

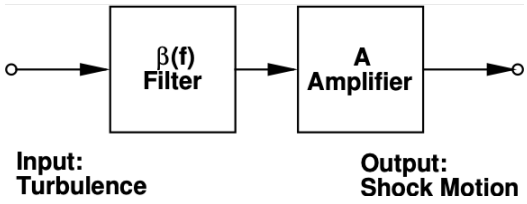


(b) Amplifier model: selective disturbance intensification.

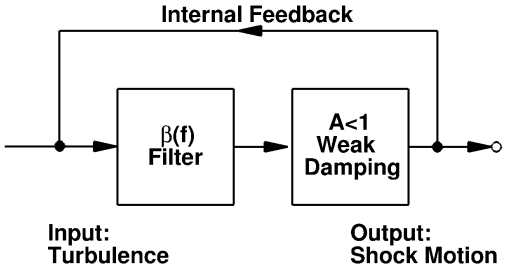


(c) Damped resonator: input stimulates decaying oscillations.

Figure 1: Conceptual models of separation unsteadiness in compressible flow. Parts (a) and (b) from Poggie et al. (2015); (c) new figure.

# 1 Introduction

Huerre and Monkewitz (1990) described the qualitative behavior of general flow instabilities in terms of convective / local instabilities (selective amplifiers) and absolute / global instabilities (self-excited oscillators). Canonical laminar-turbulent transition is an example of amplifier behavior (Fedorov, 2011). Periodic vortex shedding in a cylinder juncture flow (Visbal, 1991) is an example of oscillator behavior. Huerre and Monkewitz also described a borderline case, in which an incipient absolute instability is present. Such a flow is sensitive to inputs (external or from other instabilities via nonlinear mechanisms) that match the weakly-damped global mode, thus displaying both amplifier and oscillator characteristics. The borderline case will be called a damped resonator in the current discussion.

Large-scale separation unsteadiness is thought to originate in an instability of the separation region, but opinion is divided in the literature between the oscillator and amplifier models. Conceptual models to explain separation unsteadiness are shown schematically in Fig. 1. Under the self-excited oscillator model (Fig. 1a), the separated region moves on its own. Under the selective amplifier model (Fig. 1b), the separation region amplifies disturbances in the incoming turbulent flow that are near the same scale, but does not respond to smaller structures. The borderline case (Fig. 1c) is similar to that shown in Fig. 1b, but the unsteadiness is not self-sustaining. An analogy for this case is a bell that sounds when struck, but absent additional inputs, the ringing slowly dies out over time.

Researchers have attempted to determine the nature of separation unsteadiness through analysis of data obtained from numerical simulations and experiments. This has involved extremely involved data reduction procedures. Both passive and active flow control methods have been applied to separation control. These have been met with mixed success, because the nature of the separation unsteadiness is unknown, and flow

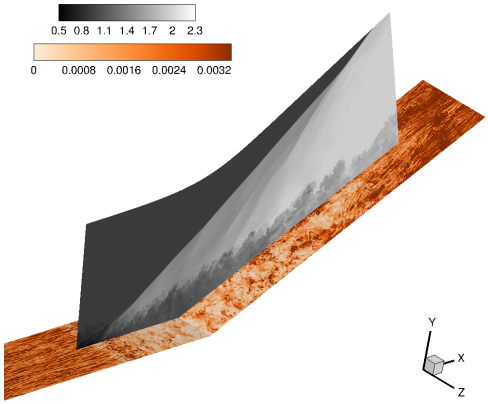


(a) Instantaneous density field $\rho/\rho_\infty$ in center plane (grayscale) and instantaneous skin friction magnitude $c_f$ at the wall (orange).

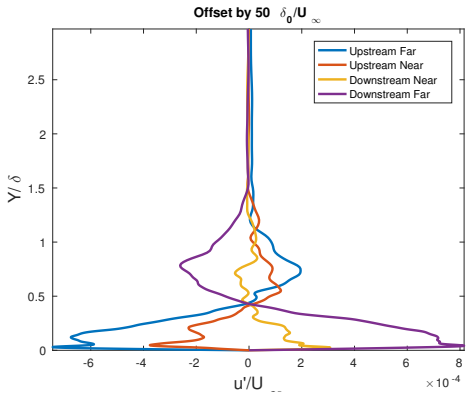


(b) Conditional averages of velocity perturbation $\hat{u}(y, t-\tau)$ with shock position $X_s(t)$ for delay $U_\infty \tau/\delta_0 = 50$.

Figure 2: Results from simulations of the compression ramp flow.

control approaches have been developed by intuition and guesswork.

The context of the amplifier and the oscillator models provides theoretical guidance for both identifying the cause of separation unsteadiness and altering it through active flow control. Under this project, we aimed to identify the primary mechanism, and then tried to modify the unsteadiness with flow control. As discussed in the next section, we were able to demonstrate upstream influence in a compression ramp flow, and alter the separation unsteadiness through periodic forcing with spatial modulation that matched a form identified through conditional averaging in the unforced flow. We expanded the scope of the investigation to include the effects on the compression ramp flow of confinement by sidewalls, and found a significant effect.

# 2 Summary of Accomplishments

Key results of the project included proof of upstream influence in a compression ramp flow (Porter and Poggie, 2019), demonstration of selective response of compression ramp flow to controlled upstream disturbances (Poggie, 2019), and demonstration of sidewall effects in a confined interaction (Poggie and Porter, 2019). Results from each of these studies are summarized next.

## 2.1 Upstream Influence in a Compression Ramp Flow

A study by Porter and Poggie (2019) of the shock-wave / boundary-layer interaction induced by a compression ramp was carried out using high-fidelity simulations. The objective was to investigate the influence of upstream disturbances on low-frequency separation unsteadiness. Two computations were performed for a 24° compression ramp at Mach 2.25, one highly resolved case and one reduced-resolution case. The reduced-resolution case was run for an extended duration to capture many cycles of low-frequency unsteadiness.

A example of the instantaneous flowfield for the high-resolution case is shown in Fig. 2a. Two planes are shown: the center plane and the no-slip wall at the bottom of the domain. In the center plane, grayscale contours of the instantaneous density field are shown. The turbulent boundary layer appears as the irregular dark region (low density) at the bottom of the plane. The primary oblique shock appears as the dark-to-light

transition in the region away from the wall. Additional weak shocks are present, along with sound radiated from the turbulent boundary layer. At the wall, the orange contours show the instantaneous magnitude of the skin friction (nondimensional magnitude of the surface force vector). Darker colors indicate higher skin friction, and instantaneous separation is apparent as a light region upstream of the corner. The separated region contains patches of high and low skin friction.

Basic flow characteristics, including statistics on the boundary layer, wall pressure, and skin friction, were computed. Frequency spectra were calculated to confirm the presence of low-frequency unsteadiness. The results showed that the reduced-resolution calculation gave physically reasonable results, albeit with a smaller separation bubble length scale than the well-resolved case.

The influence of upstream disturbances on large-scale separation unsteadiness was investigated using correlations and conditional averaging based on the position of the primary separation shock. Low-frequency unsteadiness was found to be related to structures near the wall with a time scale greater than $20\,\delta/U_\infty$, whereas the higher frequency separation motion could be attributed to turbulent boundary layer structures with a time scale on the order of $\delta/U_\infty$. These results are in qualitative agreement with the experimental results of Beresh et al. (2002).

In order elucidate the physical meaning of the correlations related to long-duration events in the incoming turbulent boundary layer, conditional averages were computed. First, the separation shock position time-history was sorted into quadrants: upstream far, upstream near, downstream near, and downstream far. Depending on the bin in which the shock position lay, the velocity at a particular delay time $\hat{u}(y, t-\tau)$ was sorted and averaged. Figure 2b shows the results for a delay of $U_\infty\tau/\delta_0 = 50$, corresponding approximately to the peak in correlations of low-pass filtered data. A distinct pattern in the boundary layer streamwise velocity fluctuations is seen to precede movement of the separation shock. When the shock is upstream, the velocity in the boundary layer tends to be low, whereas the converse is true when the shock is downstream. These results support the conclusions of Beresh et al.: an instantaneously fuller boundary layer profile is more resistant to separation. A direct effect of incoming disturbances on the shock motion is apparent, contrasting with the predictions of an oscillator model of separation unsteadiness. Since the disturbances are not observed to grow in amplitude, the amplifier model is not a good match to the behavior. The damped resonator model (Fig. 1c) seems the most appropriate qualitative description of separation unsteadiness in this flow.

## 2.2 Selective Response to Upstream Disturbances

Flow control, in the form of a time-harmonic streamwise body force with a wall-normal profile similar to the conditionally-averaged velocity profile shown in Fig. 2b, was applied to the compression ramp flow by Poggie (2019).

Figure 3 shows examples of the instantaneous flowfield for one of the cases studied. As in Fig. 2a, the orange contours show the instantaneous skin friction magnitude at the wall, and the grayscale contours show the density field in a side plane ($z = 0$). The 24° ramp begins at $x/\delta_0 = 100$; this station is labeled in the figures. An instant where the forcing term is near its positive peak is shown in Figure 3a; the effect of forcing is evident as the dark band near $x/\delta_0 = 80$ at the wall (note the labels in the figures). A corresponding instant for the negative peak is shown in Figure 3b; note the corresponding light band near $x/\delta_0 = 80$. This level of forcing is seen to cause a modest perturbation of the flow, and separation location does seem to vary in phase with the forcing function. Movies for each case corresponding to the field of view of Figure 3 are available at `https://engineering.purdue.edu/~jpoggie/forced/`.

Variables representing the instantaneous separation location $x_p(t)$ and instantaneous separation shock location $x_s(t)$ were obtained by spanwise averaging the instantaneous field at the wall and thresholding the result. Phase-averaged results for one of the forcing cases are shown in Figure 4. The behavior of the two parameters in the presence of forcing is similar. The separation location (blue line, Figure 4a) was phase locked to the forcing, with a somewhat shifted maximum relative to that observed for the separation shock

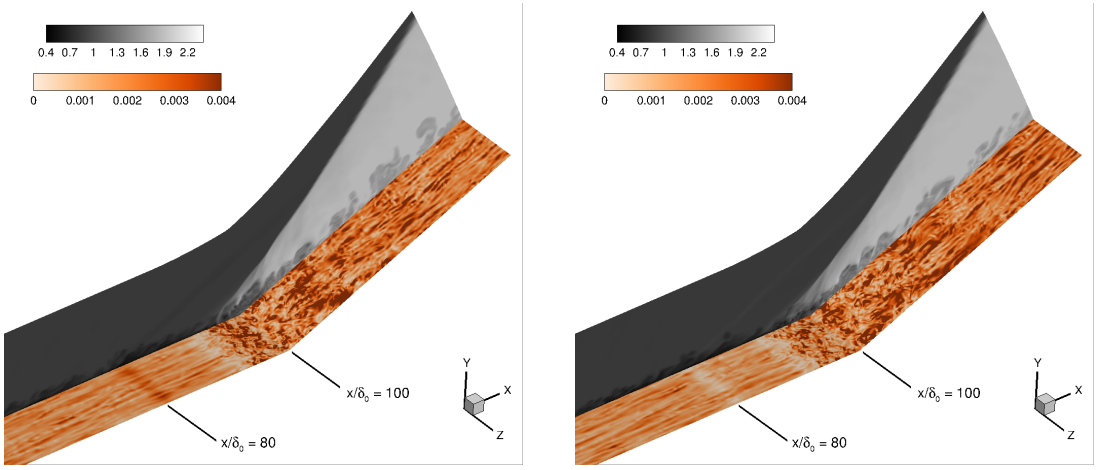


(a) Peak downstream force.

(b) Peak upstream force.

Figure 3: Examples of instantaneous flow for one of the forcing cases. Orange contours: skin friction magnitude at the wall. Grayscale contours: density in the $z = 0$ plane.

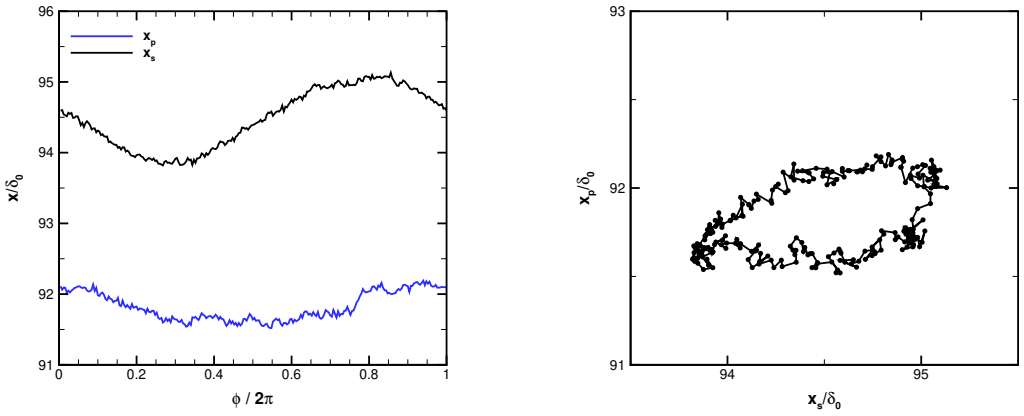


(a) Phase plot.

(b) Polar plot.

Figure 4: Phase-averaged separation location $x_p$ and shock position $x_s$ for one forcing case.

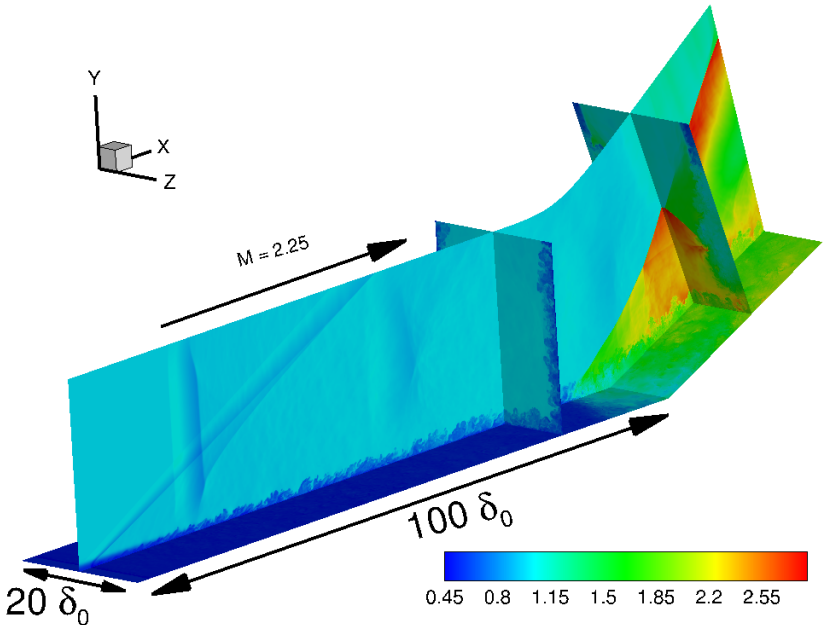


Figure 5: Overview of flow field: instantaneous density field in several planes.

(black line). A plot of $x_p$ vs. $x_s$ (Figure 4b) illustrates the relationship of the variables: the closed trajectory in the the $x_s$–$x_p$ indicates that the two variables are phase locked.

For a level of forcing that did not have a detectable effect on the mean flow in the separation region [see Poggie (2019)], significant changes were observed in the instantaneous flow. A frequency component corresponding to the forcing appeared in wall pressure spectra from a station in the separated region, and the amplitude of that peak increased with the amplitude of the forcing. The motion of the separation location and separation shock were found to be phase locked with the forcing. These results are consistent with the borderline damped resonator case (Fig. 1c) outlined by Huerre and Monkewitz (1990), a weakly-damped global mode that requires continuous input for persistant unsteadiness.

## 2.3 Effects of Flow Confinement by Sidewalls

In past work, both experimental and computational research have emphasized quasi-two-dimensional interactions. The effect of confining sidewalls can be minimized through open boundaries, aerodynamic fences, and periodic boundary conditions. Nonetheless, sidewall effects can be very important in applications such as inlet flows. It is reasonable to hypothesize that corner flows at sidewall junctures can influence separation unsteadiness, for example providing a subsonic region for upstream propagation of disturbances.

Numerical simulations were carried out by Poggie and Porter (2019) to examine the effect of sidewalls on a Mach 2.25, 24° compression ramp interaction in which the confinement effect was very strong. Inflow conditions and ramp angle were chosen to match previous simulations, and thus explore the effect of the domain width parameter on the flow structure.

An overview of the flowfield in the presence of sidewalls is shown in Figure 5, which displays the instantaneous density field in several planes. These planes include the floor of the computational domain (minimum $y$-coordinate), the centerplane ($z/\delta_0 = 10$), a plane representative of the developed, incoming turbulent boundary layer ($x/\delta_0 = 80$), and a plane normal to the ramp ($x/\delta_0 \approx 111$). The inlet flow lies at the

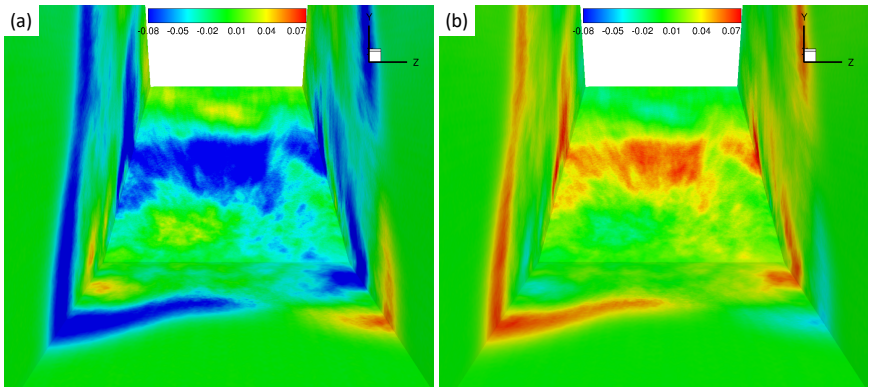


Figure 6: Deviation from overall mean for conditional averages of the pressure field. Field of view looking downstream toward the ramp. (a) High pressures on the right side (40.5% of samples). (b) Complementary average (59.5% of samples).

lower left in the figure ($x/\delta_0 = 0$). As indicated, the domain is $20\delta_0$ wide and the corner of the ramp lies at $x/\delta_0 = 100$. The laminar boundary imposed at the inlet is allowed to develop downstream until it reaches an imposed body-force trip at $x/\delta_0 = 2.5$. Weak waves from the trip are evident in the centerplane density field. Waves from the sidewall trips intersect the centerplane, as do wave reflections further downstream. A turbulent boundary layer is seen to develop on the three no-slip boundaries of the domain (irregular, dark blue contour at $x/\delta_0 = 80$). A complex shock-wave / boundary-layer interaction occurs as the boundary layer encounters the strong pressure gradient introduced by flow turning at the ramp.

The ratio of turbulent boundary layer thickness to domain width at the start of the interaction was $\delta/w = 0.12$, close to the limit of flow choking, and the overall flow structure was found to be complex. A region near the centerline of the domain resembled a two-dimensional compression ramp flow in structure. Nonetheless, this region was very narrow, confined by sidewall flows that resembled fin interactions.

The instantaneous flow was found to be intensely unsteady; animations of the behavior are available at https://engineering.purdue.edu/~jpoggie/sidewalls/. Separation and reattachment moved significantly in the streamwise direction, and reattachment was characterized by unsteady streamwise structures along the ramp. Very intense fluctuations in pressure and skin friction occurred in the corners along the ramp, with additional maxima near centerline separation and reattachment.

Although the mean flowfield is symmetric, the instantaneous flowfield can be highly asymmetric. Large-scale symmetric and antisymmetric motions of the separation zone were examined using conditional averaging. Figure 6 shows the results obtained for a condition signal corresponding to high pressures on the right side of the domain (from a viewpoint looking downstream). The contours show the deviation of the conditional average from the overall average. The results for high pressures on the right are shown in Figure 6a, and the complementary average (condition not true) is shown in Figure 6b. The condition was true for 40.5% of the samples: there was high pressure on the right side almost half the time. The results for these conditional averages seem to be consistent with an antisymmetric left-right motion of the shock system. When pressures increase on one side of the domain, they decrease on the other side.

This result, and other conditional averages, highlighted large-scale symmetric and antisymmetric modes of the separation zone. The results do not stem from spurious correlation: they identify frequent events, and consistent flow changes are observed away from the condition region.

Deshpande and Poggie (2020b,c) report on more extensive exploration of frequency spectra, cross-spectra, and cross-correlations for the same flowfield. Fourier analysis of wall pressure data revealed frequency bands

typically associated with low-frequency shock oscillations (order St = 0.01), as well as possible vortex shedding occurring at middle frequencies (order St = 0.1). The centerline shock oscillations were found to be correlated with the breathing motion of the centerline separation bubble and with turbulence in the upstream boundary layer. Coherence between shock motion and pressure fluctuations in the domain indicated asymmetric motion of the interaction, possibly caused by alternating breathing motion of the separated zones on the sidewalls. Space-time correlations on the floor suggested a strong influence of centerline separation on the corner separations and vice-versa. Similar correlations with left and right sidewalls confirmed the asymmetric motion of the interaction with a frequency of St $\approx$ 0.026.

With the presence of sidewalls, the compression ramp interaction becomes a more complex system, with additional modes of large-scale unsteadiness at different scales. Some of these modes respond to upstream disturbances, whereas others appear to oscillate on their own. Shock-wave / boundary-layer interactions in applications are expected to show a mix of oscillator (Fig. 1a) and damped resonator (Fig. 1c) behavior.

# 3 Summary and Discussion

The key results of the project were proof of upstream influence in a compression ramp flow (Porter and Poggie, 2019), demonstration of selective response of a compression ramp flow to controlled upstream disturbances (Poggie, 2019), and demonstration of sidewall effects in a confined interaction (Poggie and Porter, 2019).

The finding that the separation region responds selectively to large-scale, near-wall perturbations in the incoming flow supports a model of separation unsteadiness in which external forcing by boundary layer turbulence drives a weakly-damped global mode of the separation bubble. This is the intermediate case (Fig. 1c) between the amplifier and oscillator models. This outlook contrasts with the view that the separation region oscillates on its own, or with a view that a growing instability drives the unsteadiness.

The present results are consistent with previous theoretical and computational work (Plotkin, 1975; Pirozzoli et al., 2010; Touber and Sandham, 2011; Martin et al., 2016; Nichols et al., 2017). If the separation bubble possesses a weakly-damped global mode, then a number of seemingly contradictory observations are explained. The success of the Plotkin (1975) model in predicting the spectrum (Poggie and Smits, 2001, 2005; Poggie et al., 2015) reflects the response of a weakly-damped global mode to external forcing. The assertions that upstream and downstream fluctuations are connected to the separation bubble motion are both correct: the system responds to whatever disturbances are present. The lack of straightforward correlation between separation motion and turbulent fluctuations is a result of a selective response to perturbations that match the global mode. Thus the weakly-damped global mode model reconciles debates between amplifier / oscillator models and upstream / downstream mechanisms of separation unsteadiness.

An interesting possibility is that, under the right change in flow conditions, the global mode could move into an undamped regime, and the system might start to oscillate on its own. Such behavior has been observed previously in low-speed juncture flows (Visbal, 1991). Our research group has observed oscillator-like behavior at high Mach number in detached eddy simulations of a reattaching shear layer (Leger et al., 2017; Deshpande and Poggie, 2020b) and an elevon-cove flow (Alviani et al., 2020). (In detached eddy simulation, only the mean flow is modeled for the incoming boundary layer. There are no incoming disturbances imparted on the separated region, so any unsteadiness must be a result of a downstream mechanism.)

Some authors (Martin et al., 2016; Adler and Gaitonde, 2018) have concluded that that the low-frequency separation motion is insensitive to external forcing. This may be the case for some conditions, but it is not universally true. Poggie (2019) presents an example of a flow where separation motion is directly driven by external forcing. Although the generality of the result remains to be seen, large-scale separation motion in the present flow responds to external disturbances of a certain form, which was identified through conditional averaging of the undisturbed flow. These results support the conclusions of the experimental study by Beresh

et al. (2002).

The path to flow control would appear to entail matching actuator-induced perturbations to the global mode of the separation bubble. It would be of interest to map out the transfer function of the forcing, and examine the sensitivity of the flow response to the spatial form of the forcing function. Various methods of modal decomposition could be used to identify the required form, and phased arrays of actuators could be used to provide the needed inputs. It might also be possible to carry out experiments for direct comparison with the present approach using a slot blowing device or a magnetohydrodynamic actuator.

The influence of sidewalls on shock-wave / boundary-layer interactions is seen to be significant, and this effect is worthy of additional research attention. Subsonic corner flows offer a path for upstream propagation of disturbances that is expected to influence unsteadiness in many practical situations. In ongoing work, we are examining the spectrum and coherence of fluctuations at the wall and in the corners of the flow, and are applying modal decomposition techniques to this data set. The results will be presented by Deshpande and Poggie at the 2021 AIAA SciTech Conference.

# 4 List of Publications

## 4.1 Conference Papers

1. Porter and Poggie (2017)
2. Deshpande and Poggie (2017)
3. Deshpande and Poggie (2018b)
4. Poggie and Porter (2018)
5. Hall and Poggie (2019)
6. Deshpande and Poggie (2019a)
7. Piskin et al. (2019a)
8. Deshpande and Poggie (2019b)
9. Deshpande and Poggie (2020a)

## 4.2 Journal articles

1. Agostini et al. (2017)
2. Leger et al. (2017)
3. Srinivasan et al. (2018)
4. Gutiérrez and Poggie (2018)
5. Deshpande and Poggie (2018a)
6. Porter and Poggie (2019)
7. Poggie and Porter (2019)
8. Poggie (2019)

9. Piskin et al. (2019b)
10. Deshpande and Poggie (2020b)
11. Deshpande and Poggie (2020c)

### 4.3 MS Theses and PhD Dissertations

1. Deshpande (2017)
2. Porter (2017)
3. Srinivasan (2017)
4. Hall (2019)
5. Piskin (2019)

## 5 Personnel Supported

Professors Jonathan Poggie and Sergey Macheret received summer salary support under this grant. Kevin Porter was supported for his master's degree, and Akshay Deshpande was supported for a portion of his master's and doctoral degrees.

The following students carried out work for the project, but received support from other sources: David Gutiérrez (unfunded undergraduate student), Ian Hall (SMART scholarship), Tugba Piskin (Purdue teaching assistant), Sashank Srinivasan (Purdue teaching assistant).

## References


M. C. Adler and D. V. Gaitonde. Dynamic linear response of a shock / turbulent-boundary-layer interaction using constrained perturbations. *Journal of Fluid Mechanics*, 840:291–341, 2018. URL https://doi.org/10.1017/jfm.2018.70.

L. Agostini, M. Leschziner, J. Poggie, N. Bisek, and D. Gaitonde. Multi-scale interactions in a compressible boundary layer. *Journal of Turbulence*, 18(8):760–780, 2017. URL https://doi.org/10.1080/14685248.2017.1328108.

R. Alviani, J. Poggie, and G. Blaisdell. Detached eddy simulation of supersonic wing-elevon cove boundary-layer ingestion. AIAA Paper 2020-3008, American Institute of Aeronautics and Astronautics, Reston VA, June 2020. URL https://doi.org/10.2514/6.2020-3008.

S. J. Beresh, N. T. Clemens, and D. S. Dolling. Relationship between upstream turbulent boundary-layer velocity fluctuations and separation shock unsteadiness. *AIAA Journal*, 40(12):2412–2422, 2002. URL https://doi.org/10.2514/2.1609.

A. S. Deshpande. Supersonic flow control of swept shock wave / turbulent boundary layer interaction using plasma actuators. Master's thesis, Purdue University, West Lafayette IN, August 2017.

A. S. Deshpande and J. Poggie. Supersonic flow control of swept shock wave / turbulent boundary layer interactions using plasma actuators. AIAA Paper 2017-3479, American Institute of Aeronautics and Astronautics, Reston VA, June 2017. URL https://doi.org/10.2514/6.2017-3479.

A. S. Deshpande and J. Poggie. Flow control of swept shock-wave / boundary-layer interaction using plasma actuators. *Journal of Spacecraft and Rockets*, 55(5):1198–1207, 2018a. URL https://doi.org/10.2514/1.A34114.

A. S. Deshpande and J. Poggie. Effects of curvature in high speed inlets. AIAA Paper 2018-3393, American Institute of Aeronautics and Astronautics, Reston VA, June 2018b. URL https://doi.org/10.2514/6.2018-3393.

A. S. Deshpande and J. Poggie. Unsteadiness in a compressible reattaching shear layer. AIAA Paper 2019-1874, American Institute of Aeronautics and Astronautics, Reston VA, January 2019a. URL https://doi.org/10.2514/6.2019-1874.

A. S. Deshpande and J. Poggie. Statistical analysis of unsteadiness in a compressible reattaching flow. AIAA Paper 2019-3439, American Institute of Aeronautics and Astronautics, Reston VA, June 2019b. URL https://doi.org/10.2514/6.2019-3439.

A. S. Deshpande and J. Poggie. Unsteadiness of shock-wave / boundary-layer interaction with sidewalls. AIAA Paper 2020-0581, American Institute of Aeronautics and Astronautics, Reston VA, January 2020a. URL https://doi.org/10.2514/6.2020-0581.

A. S. Deshpande and J. Poggie. Unsteady characteristics of compressible reattaching shear layers. *Physics of Fluids*, 32:066103, 2020b. URL https://doi.org/10.1063/5.0008752.

A. S. Deshpande and J. Poggie. Large-scale unsteadiness in a compression ramp flow confined by sidewalls. *Physical Review Fluids*, 2020c. Submitted for revision review, 2020-10-13.

A. Fedorov. Transition and stability of high-speed boundary layers. *Annual Review of Fluid Mechanics*, 43: 79–95, 2011. URL https://doi.org/10.1146/annurev-fluid-122109-160750.

D. R. Gutiérrez and J. Poggie. Effects of power deposition on the aerodynamic forces on a slender body. *AIAA Journal*, 56(7):2911–2917, 2018. URL https://doi.org/10.2514/1.J057004.

I. Hall. Simulating scramjet behavior: Unstart prediction in a supersonic, turbulent inlet-isolator duct flow. Master's thesis, Purdue University, West Lafayette IN, May 2019.

I. A. Hall and J. Poggie. Simulation of unstart in hypersonic flow with a dual-mode scramjet model. AIAA Paper 2019-0946, American Institute of Aeronautics and Astronautics, Reston VA, January 2019. URL https://doi.org/10.2514/6.2019-0946.

P. Huerre and P. A. Monkewitz. Local and global instabilities in spatially developing flows. *Annual Review of Fluid Mechanics*, 22:473–537, 1990. URL https://doi.org/10.1146/annurev.fl.22.010190.002353.

T. Leger, N. Bisek, and J. Poggie. Detached-eddy simulation of a supersonic reattaching shear layer. *AIAA Journal*, 55(11):3722–3733, 2017. URL https://doi.org/10.2514/1.J056103.

M. P. Martin, S. Priebe, and C. M. Helm. Upstream and downstream influence on STBLI instability. AIAA Paper 2016-3341, American Institute of Aeronautics and Astronautics, Reston VA, June 2016. URL https://doi.org/10.2514/6.2016-3341.

J. W. Nichols, J. Larsson, M. Bernardini, and S. Pirozzoli. Stability and modal analysis of shock / boundary layer interactions. *Theortical and Computational Fluid Dynamics*, 31:33–50, 2017. URL https://doi.org/10.1007/s00162-016-0397-6.

S. Pirozzoli, J. Larsson, J. W. Nichols, M. Bernardini, B. E. Morgan, and S. K. Lele. Analysis of unsteady effects in shock/boundary layer interactions. In P. Moin, J. Larsson, and N. Mansour, editors, *Studying Turbulence Using Numerical Simulation Databases*, volume XIII of *Proceedings of the CTR Summer Program*, pages 153–164, Stanford, CA, December 2010. Center for Turbulence Research, Stanford University. URL https://web.stanford.edu/group/ctr/Summer/SP10/2_10_pirozzoli.pdf.

T. Piskin. *Numerical Simulation of Gas Discharges for Flow Control Applications*. PhD thesis, Purdue University, West Lafayette IN, August 2019.

T. Piskin, S. O. Macheret, and J. Poggie. Effect of local field approximation in simulations of gas discharges. AIAA Paper 2019-3356, American Institute of Aeronautics and Astronautics, Reston VA, June 2019a. URL https://doi.org/10.2514/6.2019-3356.

T. Piskin, V. A. Podolsky, S. O. Macheret, and J. Poggie. Challenges in numerical simulation of nanosecond-pulse discharges. *Journal of Physics D: Applied Physics*, 52:304002, 2019b. URL https://doi.org/10.1088/1361-6463/ab1fbe.

K. J. Plotkin. Shock wave oscillation driven by turbulent boundary-layer fluctuations. *AIAA Journal*, 13(8): 1036–1040, 1975. URL https://doi.org/10.2514/3.60501.

J. Poggie. Effect of forcing on a supersonic compression ramp flow. *AIAA Journal*, 57(9):3765–3772, 2019. URL https://doi.org/10.2514/1.J058504.

J. Poggie and K. M. Porter. Numerical simulation of sidewall influence on supersonic compression ramp interactions. AIAA Paper 2018-4029, American Institute of Aeronautics and Astronautics, Reston VA, June 2018. URL https://doi.org/10.2514/6.2018-4029.

J. Poggie and K. M. Porter. Flow structure and unsteadiness in a highly-confined shock-wave / boundary-layer interaction. *Physical Review Fluids*, 4:024602, 2019. URL https://doi.org/10.1103/PhysRevFluids.4.024602.

J. Poggie and A. J. Smits. Shock unsteadiness in a reattaching shear layer. *Journal of Fluid Mechanics*, 429: 155–185, 2001. URL https://doi.org/10.1017/S002211200000269X.

J. Poggie and A. J. Smits. Experimental evidence for Plotkin model of shock unsteadiness in separated flow. *Physics of Fluids*, 17:018107, 2005. URL https://doi.org/10.1063/1.1833405.

J. Poggie, N. J. Bisek, R. L. Kimmel, and S. A. Stanfield. Spectral characteristics of separation shock unsteadiness. *AIAA Journal*, 53(1):200–214, 2015. URL https://doi.org/10.2514/1.J053029.

K. M. Porter. Simulations of shock-wave / boundary-layer interaction on compression ramps. Master's thesis, Purdue University, West Lafayette IN, August 2017.

K. M. Porter and J. Poggie. Turbulence structure and large-scale unsteadiness in shock-wave / boundary layer interaction. AIAA Paper 2017-0533, American Institute of Aeronautics and Astronautics, Reston VA, January 2017. URL https://doi.org/10.2514/6.2017-0533.

K. M. Porter and J. Poggie. Selective upstream influence on the unsteadiness of a separated turbulent compression ramp flow. *Physics of Fluids*, 31:016104, 2019. URL https://doi.org/10.1063/1.5078938.

S. Srinivasan. A positivity-preserving discontinuous galerkin finite element scheme for modeling electrical discharges. Master's thesis, Purdue University, West Lafayette IN, August 2017.

S. Srinivasan, J. Poggie, and X. Zhang. A positivity-preserving high order discontinuous galerkin scheme for convection-diffusion equations. *Journal of Computational Physics*, 366:120–143, 2018. URL https://doi.org/10.1016/j.jcp.2018.04.002.

E. Touber and N. D. Sandham. Low-order stochastic modelling of low-frequency motions in reflected shock-wave / boundary-layer interactions. *Journal of Fluid Mechanics*, 671:417–465, 2011. URL https://doi.org/10.1017/S0022112010005811.

M. R. Visbal. Structure of laminar juncture flows. *AIAA Journal*, 29(8):1273–1282, 1991. URL https://doi.org/10.2514/3.10732.